

Supporting Information

A “Two-Birds-One-Stone” Strategy to Enhance Capacitive Deionization Performance of Flexible $\text{Ti}_3\text{C}_2\text{T}_x$ MXene Film Electrodes by Surface Modification

Chuhan Huang^{ab}, Tianqin Huang^{ab}, Xue Liang Li^{*c}, Wei Zhou^{ab}, and Meng Ding^{*ab}

- a. Department of Chemistry, School of Science, Xi'an Jiaotong-Liverpool University, Suzhou 215123, P. R. China.
- b. Department of Chemistry, University of Liverpool, Liverpool L69 7ZD, UK
- c. Pillar of Engineering Product Development, Singapore University of Technology and Design, 487372, Singapore

Corresponding email:

xueliang_li@sutd.edu.sg (X. Li)

Meng.Ding@xjtlu.edu.cn (M. Ding)

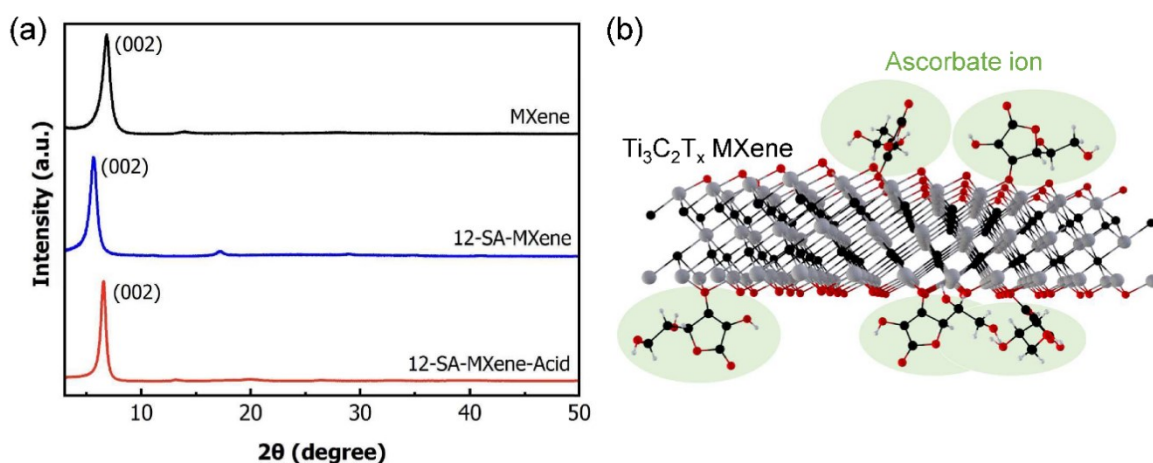


Fig. S1 (a) XRD patterns of MXene, 12-SA-MXene, and 12-SA-MXene after treatment with dilute HCl. (b) Schematic illustration of SA-MXene.

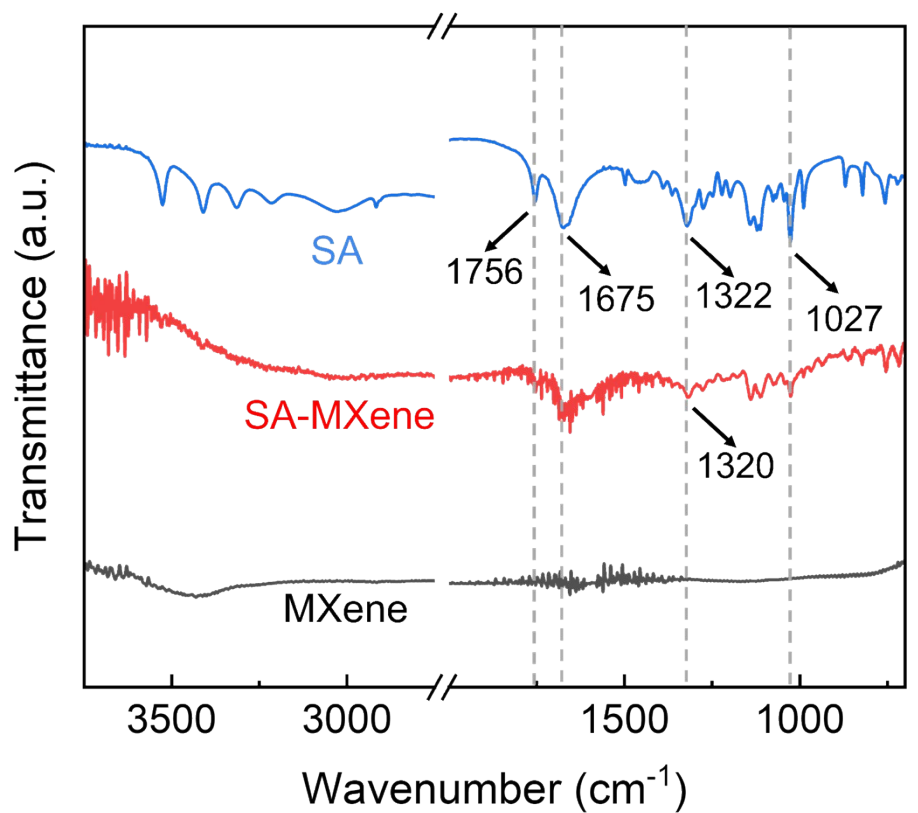


Fig. S2 FTIR spectra of SA, SA-MXene, and pristine MXene

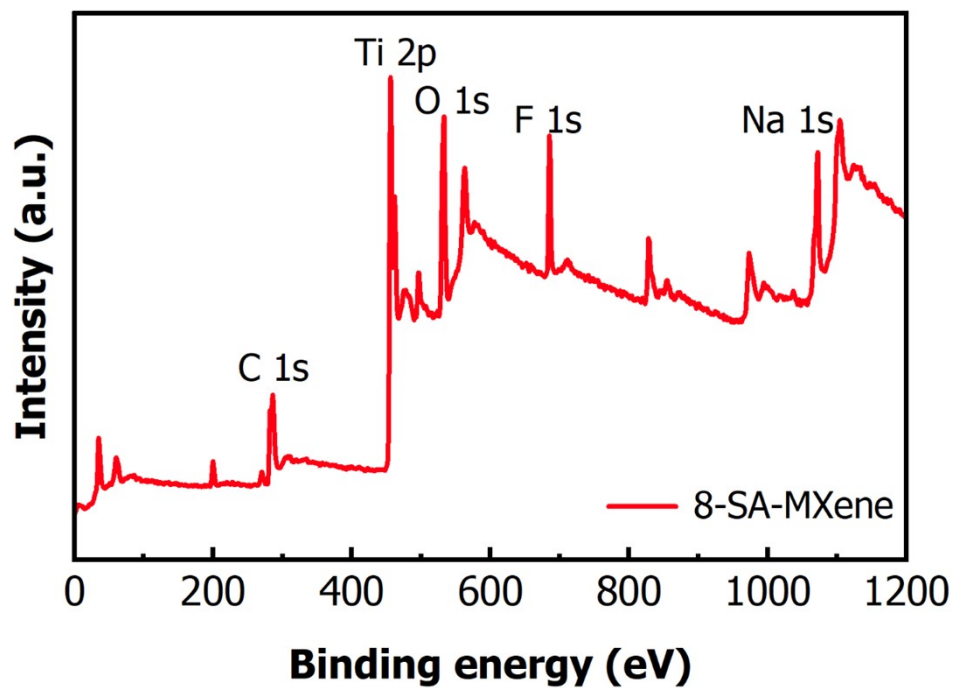


Fig. S3 XPS survey spectrum for 8-SA-MXene.

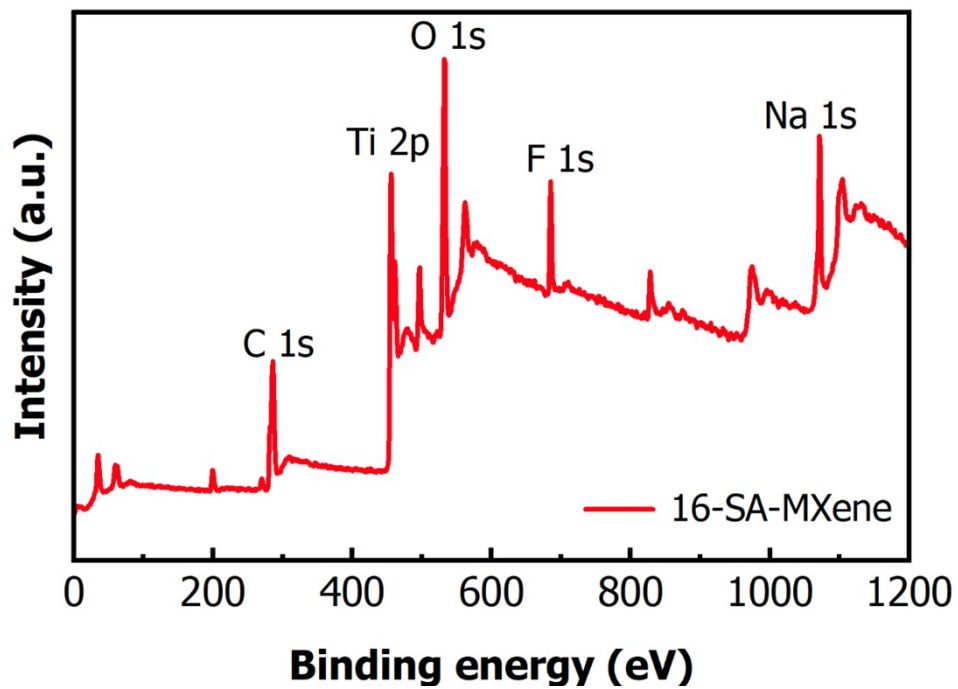


Fig. S4 XPS survey spectrum for 16-SA-MXene.

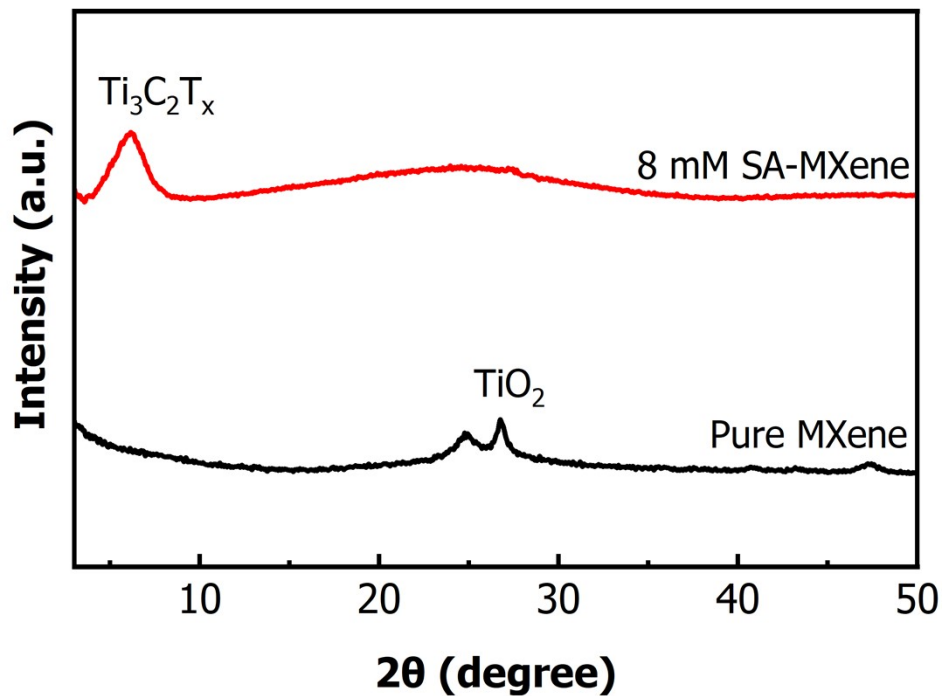


Fig. S5 XRD patterns of SA-MXene and pristine MXene after 90 days storage.

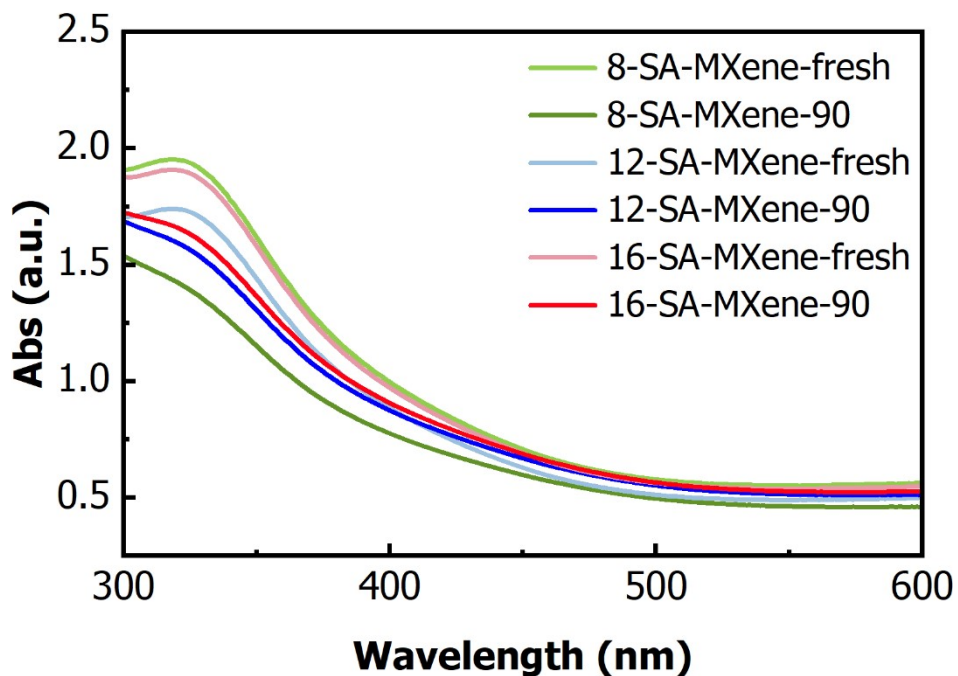


Fig. S6 UV-vis spectra of 8-SA-MXene, 12-SA-MXene and 16-SA-MXene before and after 90 days of storage.

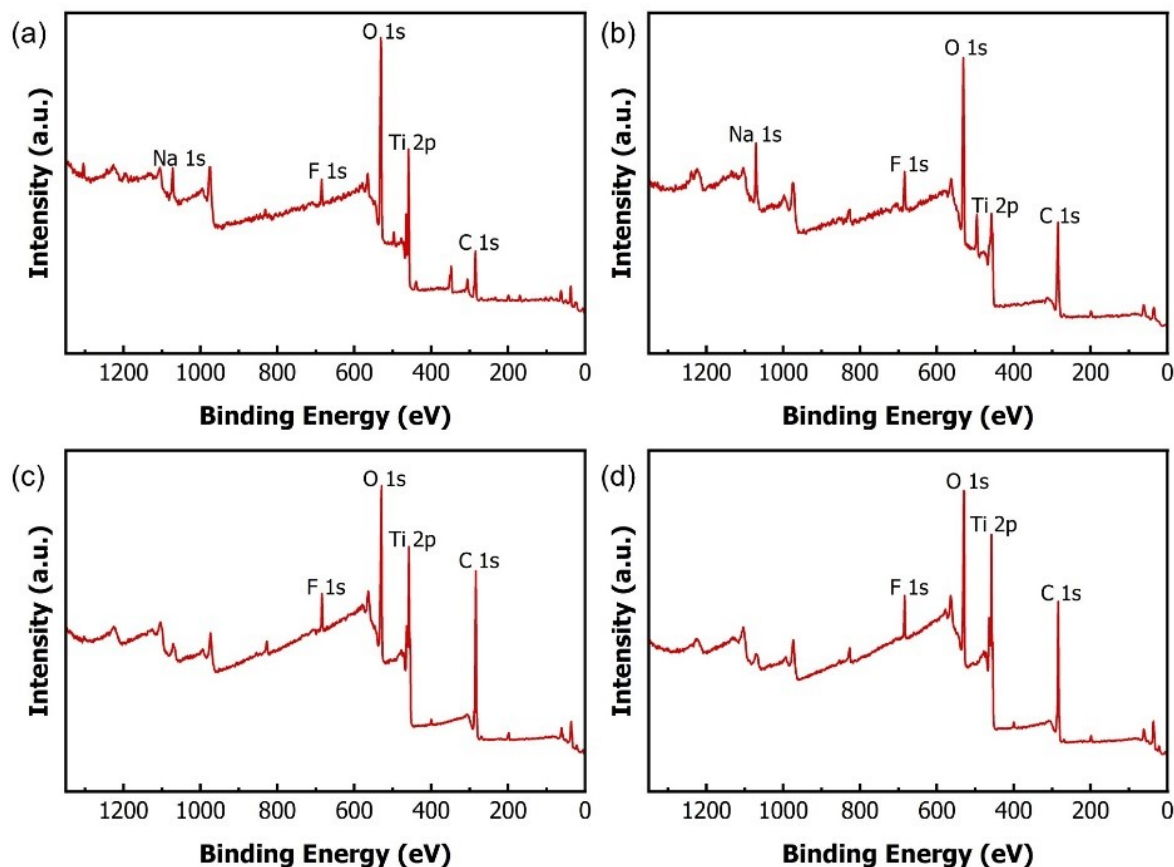


Fig. S7 XPS survey spectra of (a) pristine MXene and (b) SA-MXene after 90-days storage, as well as (a) pristine MXene and SA-MXene electrode after CDI tests.

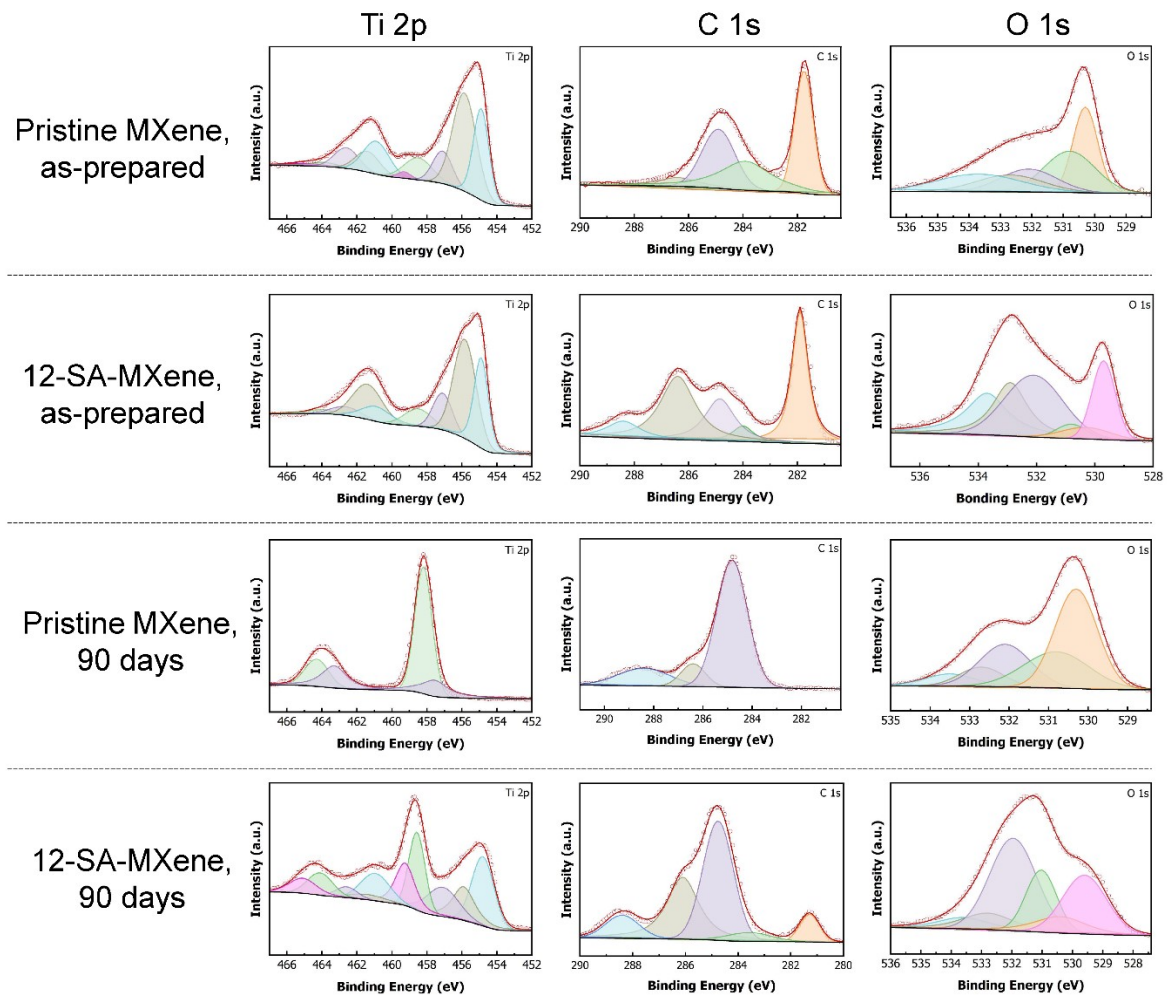


Fig. S8 Component peak fittings of XPS spectra for pristine MXene nanosheets and 12-SA-MXene nanosheets when as-prepared and after 90-days storage.

Table S1 XPS peak fitting results for as-prepared Ti₃C₂T_x MXene

Element	Binding energy (BE) (eV)	Component name
Ti 2p _{3/2} (2p _{1/2})	459.3 (464.9)	Ti-F _x
	458.5 (463.9)	TiO ₂
	457.1 (462.6)	Ti ³⁺
	455.9 (461.4)	Ti ²⁺
	454.9 (460.9)	Ti-C
O 1s	533.7	H ₂ O ^b
	532.7	Al ₂ O ₃
	532.1	C-Ti-(OH) _x
	530.8	C-Ti-O _x
	530.3	TiO ₂
C 1s	529.7	Ti-O-Ti
	281.7	C-Ti
	283.9	Ti-C-O
	284.9	C-C
	286.4	C-O
	288.4	C=O

Table S2 Comparison of component atomic percentages of as-prepared MXene and SA-MXene from the XPS peak fitting result of Ti 2p.

Samples	Component atomic percentage (%)			
	TiO ₂	Ti ³⁺	Ti ²⁺	Ti-C
As-prepared MXene	10.8%	15.5%	38.6%	31.8%
SA-MXene	9.7%	14.6%	47.5%	28.2%

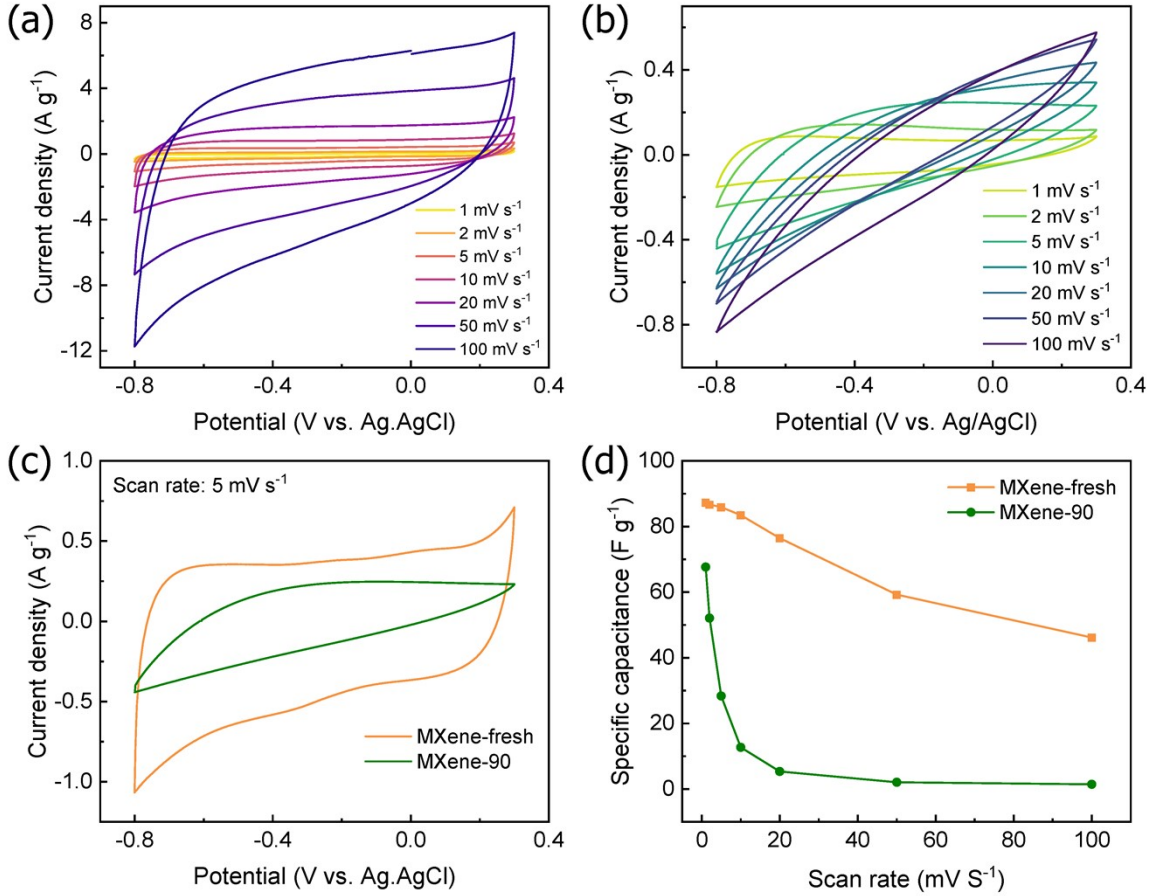


Fig. S9 (a) CV curves for MXene with scan rates varied from 1 mV s^{-1} to 100 mV s^{-1} . (b) CV curves for MXene-90 with scan rates varied from 1 mV s^{-1} to 100 mV s^{-1} . (c) CV curves for MXene and MXene-90 with scan rate of 5 mV s^{-1} . (d) Specific capacitance comparison of MXene and MXene-90 at a scan rate from 1 mV s^{-1} to 100 mV s^{-1} .

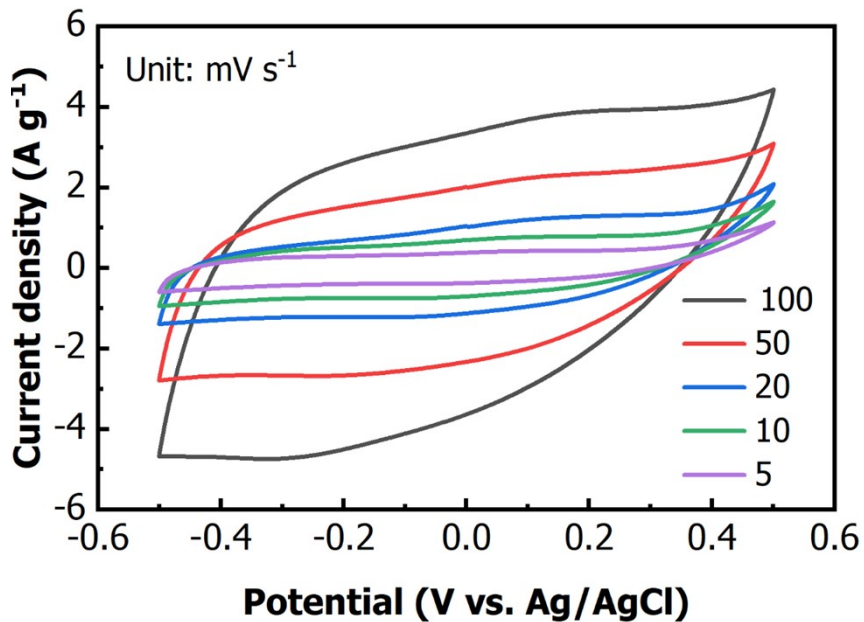


Fig. S10 CV patterns of 8-SA-MXene with scan rates varied from 5 mV s^{-1} to 100 mV s^{-1} .

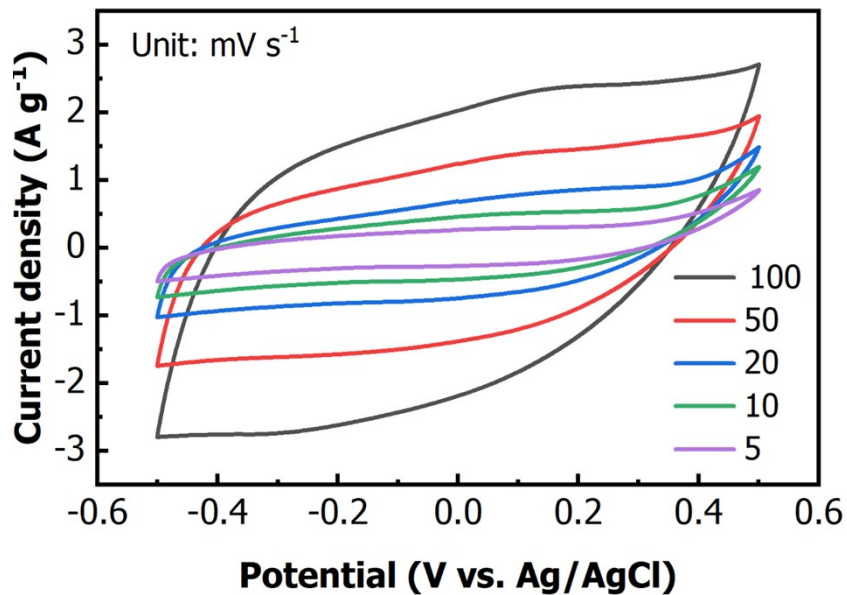


Fig. S11 CV patterns of 16-SA-MXene with scan rates varied from 5 mV s^{-1} to 100 mV s^{-1} .

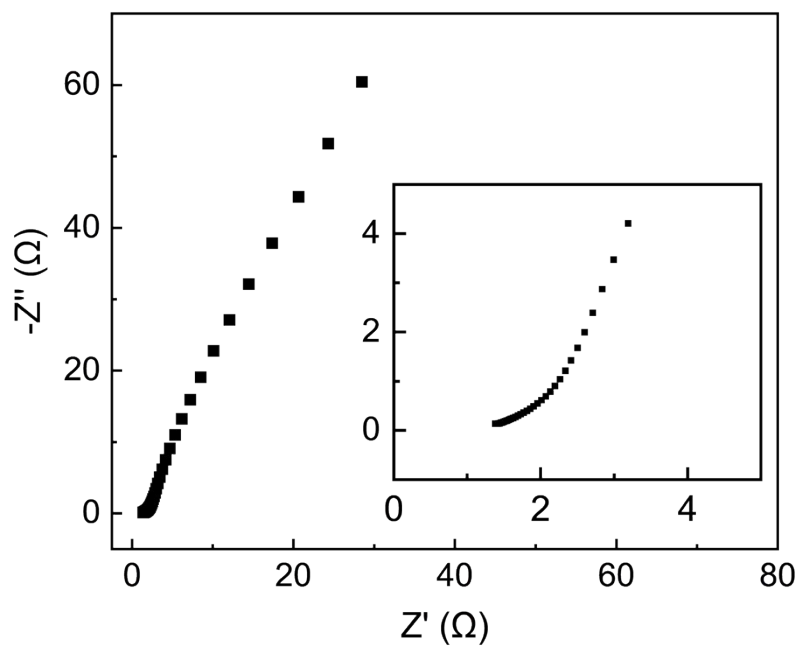


Fig. S12 Nyquist plots of pristine MXene

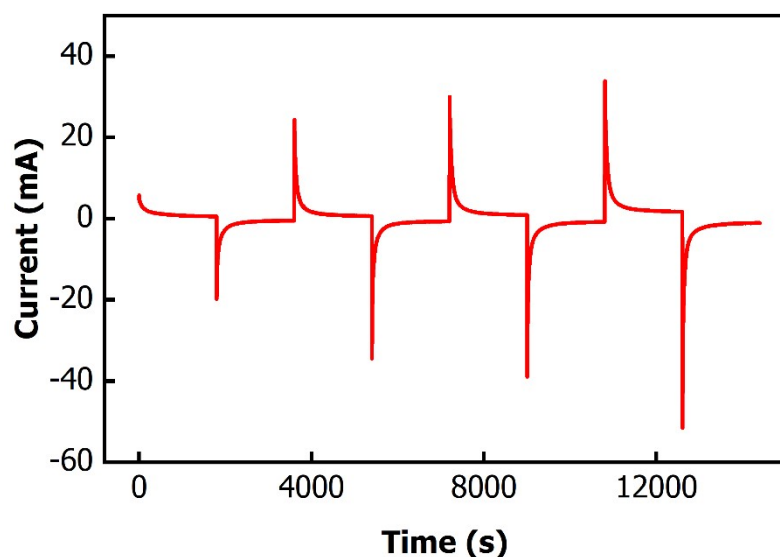


Fig. S13 The corresponding current responses in CDI processes at 1.0, 1.2, 1.4, and 1.6 V, respectively.

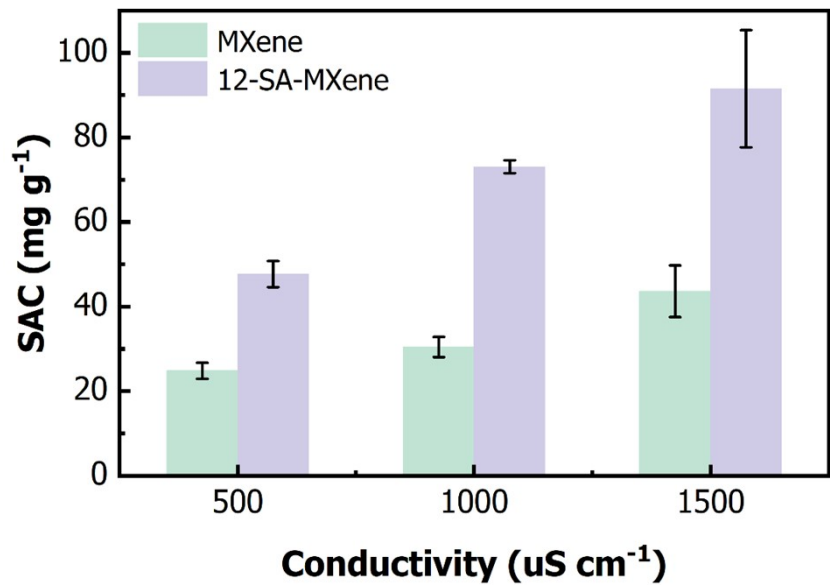


Fig. S14 Specific SAC values of pristine MXene and 12-SA-MXene electrode in different initial concentrations of NaCl feed solution.

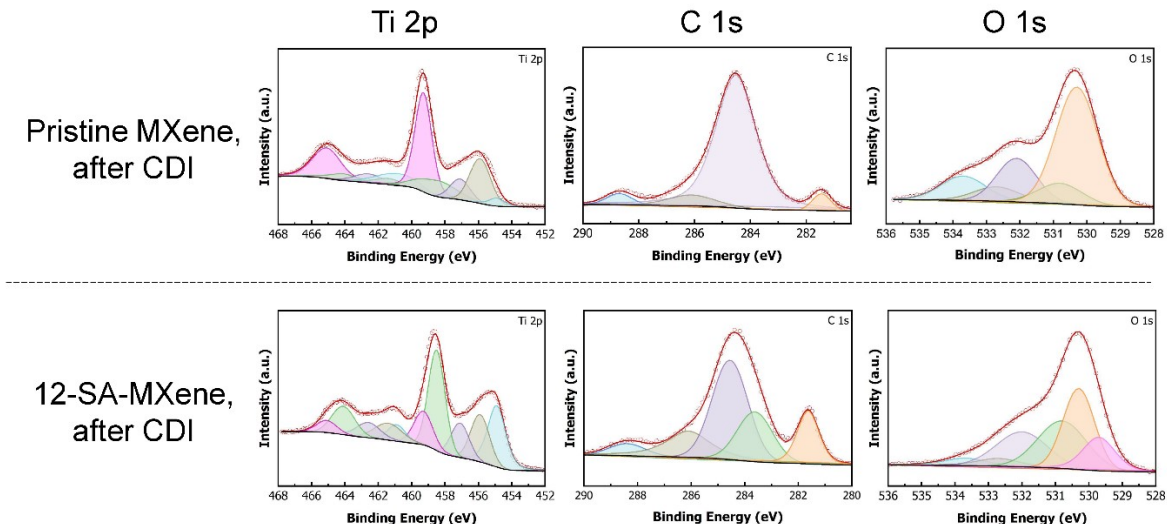


Fig. S15 XPS peak fittings for pristine MXene nanosheets and 12-SA-MXene nanosheets after CDI tests.

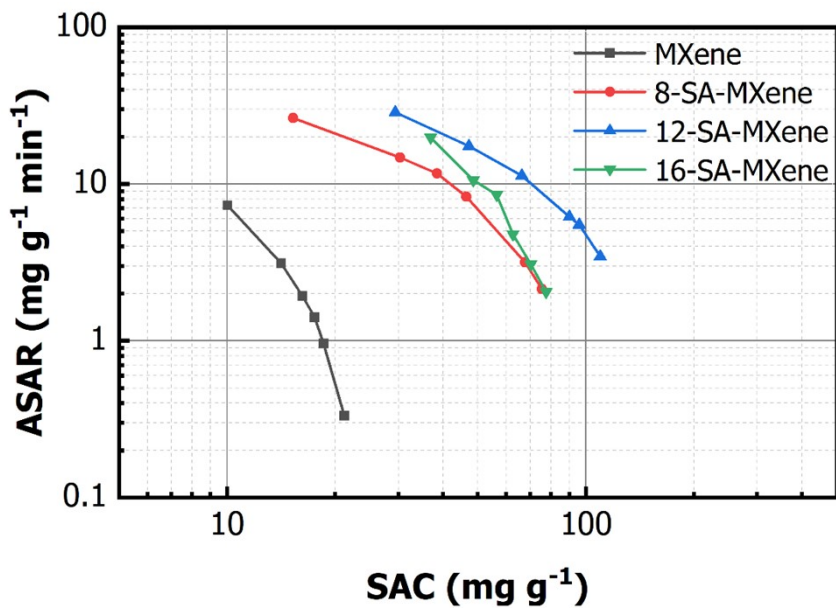


Fig. S16 CDI Ragone plot of pristine MXene, 8-SA-MXene, 12-SA-MXene and 16-SA-MXene electrodes.

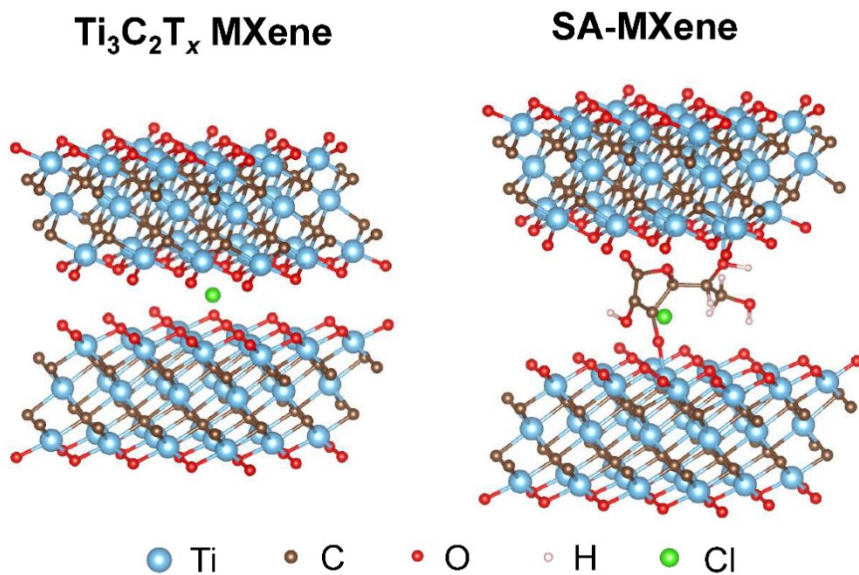


Fig. S17 Adsorption configuration of Cl on the surface of $\text{Ti}_3\text{C}_2\text{T}_x$ MXene and SA-MXene.